MOEM

Modern Electronic Materials 2022; 8(2): 65–72
DOI 10.3897/j.moem.8.2.90062

Research Article

Development of a mobile independent solar power plant based on solid-state heterojunction photocells for agricultural purposes

Serekbol Zh. Tokmoldin[1,2], Vasiliy V. Klimenov[1,2], Dmitriy V. Girin[1,2], Nikolay A. Chuchvaga[1,2], Kazybek P. Aimaganbetov[1,2], Musabek P. Kishkenebaev[2], Svetlana N. Tarakanova[2], Nurlan S. Tokmoldin[1,2]

1 Scientific Production Center of Agricultural Engineering, LTD, 312 Raiymbek Ave., Almaty 050005, Republic of Kazakhstan

2 Satbayev University, Institute of Physics and Technology, 11 Ibragimov Str., Almaty A26T9C7, Republic of Kazakhstan

Corresponding author: Nikolay A. Chuchvaga (nikolay.chuchvaga@gmail.com)

Received 5 May 2022 ♦ **Accepted** 12 June 2022 ♦ **Published** 30 June 2022

Citation: Tokmoldin SZh, Klimenov VV, Girin DV, Chuchvaga NA, Aimaganbetov KP, Kishkenebaev MP, Tarakanova SN, Tokmoldin NS (2022) Development of a mobile independent solar power plant based on solid-state heterojunction photocells for agricultural purposes. *Modern Electronic Materials* 8(2): 65–72. https://doi.org/10.3897/j.moem.8.2.90062

Abstract

Mathematical simulation of temperature distribution on double-sided solar cells has been carried out. Differences in the configuration of photoelectric converters prove to solely amount to the fact that a double-sided solar cell has a more efficient heat sink at the rear side. Furthermore double-sided solar cells exhibit higher power conversion performance. Calculations confirm the correctness of giving preference to double-sided solar cells which is of great importance for the photoelectric converter design developed by us. Analysis of market-available photovoltaic technologies of solar energy to electric power conversion has led to the development of a photovoltaic converter on the basis of double-sided silicon heterojunction solar cells. The configuration developed is a moving platform having a photovoltaic cell array mounted on it and a light flux collector.

A double-axis tracking system has been developed for the general case of planar attachment of solar cell modules. A 350 mm stroke drive provides for movement in the north-south direction and a 450 mm stroke drive, in the east-west direction. The task has been outlined to find the required arm for providing symmetrical positioning at the maximum rotation angle about the axis. As a result, technical solutions have been developed for the north-south and the east-west directions.

Furthermore a schematic wiring diagram has been designed to implement the preset solar tracking system algorithm. The system is also fitted with a GPS/GLONASS module for system precision positioning and time synchronization.

Keywords

solar power plant, HIT heterojunction technology, agriculture, photocell, photovoltaic

1. Introduction

The integration between the power industry and agriculture is intensifying both in well-developed and developing states. Social problems e.g. climate change consequences, the need for cleaner energy production and waste reduction as well as the rapid population growth and economic development have entailed a growing demand for food, water and energy. The growing energy consumption from renewable sources (wind, sun, geothermal energy, biomass, hydraulic) and their new potential agricultural application are intended to target the above-mentioned problems. Global agreements e.g. the 2015 Paris Agreement, along with the necessity of a transition to low-carbon economy and global CO_2 waste reduction predetermine the increased use of renewable energy sources. These sources replace or add to the existing ones and are used for powering the key economy segments in developing states. For example the overall capacity of renewable energy sources in India is expected to double in the period from 2016 to 2022 [1, 2].

Photovoltaics **(PV)** and wind energy are already accounting for 90% of India's power industry growth due to a major cost reduction. Furthermore renewable energy sources demonstrate record-breaking growth in other states both in the North and in the South Hemispheres (IEA 2017). For example, according to the Jordanian National Energy Strategy Plan the current share of renewable energy sources is 29.4% of the overall power production figure. Hydraulic industry is among Jordanian key energy consumers: 15% of Jordan's overall power consumption is accounted for by water pumping stations. Thus the power industry targets the use of renewable energy sources and increasing energy efficiency (Ministry of Water and Irrigation, 2016). Segments like agriculture and water supply will benefit from the use of renewable energy sources since they can replace existing ones and make relatively cheap energy available for different agricultural consumers including water heating, water extraction, crop drying, grain milling, greenhouse heating, illumination etc. [1, 2].

The dynamic growth of the share of photovoltaic systems in the energy production of many states originates from their numerous advantages including absence of environment pollution or other environmental damage. Furthermore solar generation does not produce noise, and solar energy is directly converted to electric power [3].

Resource base development through an increase in renewable energy share and a transition to alternative energy sources are among the most important tasks faced by the Republic of Kazakhstan. The agricultural segment of the Republic incorporates about 222 ths. individual households and farms, 1659 agricultural production cooperative enterprises, and 7709 economic associations of various ownership types and joint stocks.

Farms located far from central power sources face electric power deficiency. Large share of energy is consumed by illumination of production facilities and alarms, domestic electric appliances and electric equipment for power-assisted works.

The development of concentrator-based solar power industry started back in the 1970s [4]. Nowadays concentrator-based systems exhibit superior efficiency in photovoltaic power industry [5]. Further development of concentrator-based systems will reduce the consumption of semiconductors [6] thus tangibly reducing the cost factor of photocells which will be compensated by the higher efficiency of photovoltaic converters [7–9].

Analysis of market-available photoelectric technologies of solar energy to electric power conversion has led to the development of a photoelectric converter on the basis of double-sided silicon heterojunction solar cells. Preference to this type of solar cell arrays is given as a result of a solar system efficiency analysis conducted by M. Grin's team [10, 11]. The solar cell modules combine the advantages of amorphous and single crystal silicon for the achievement of high solar energy conversion efficiency (~ 25% for solar cells) and ensure lower silicon consumption coupled with process temperature reduction to within 200–250 °C [12, 13]. While exhibiting record-breaking performance [14–16], products on the basis of multi-junction photovoltaic cells are quite expensive due to the complexity of the technologies and the high cost of materials used. Alternative option for solar modules used in advanced photoelectric converters can be solar cells based on single crystal silicon (Si), gallium arsenide (GaAs) or thin films **(CIGS)** [17–19]. However silicon heterojunction photocells remain the most preferable option for consumer photovoltaic devices by the cost-to-quality criterion [20, 21].

2. Experimental methods and discussion

The key parameter describing the performance of solar radiation concentrators is the concentration coefficient which is determined as the ratio between the average density of concentrated radiation and the density of the light flux incident upon the reflecting surface. The concentrating capacity of a system is determined by the geometry of the concentrator, the angular radius of the solar disc and the reflection capacity of the mirror surface. High-power concentrator systems typically have a second-order rotation surface configuration, e.g. paraboloid, ellipsoid, hyperboloid or hemispheric shapes. These shapes deliver the highest radiation density, which is far greater than the respective solar constant [22].

The configuration developed by our team is a moving platform with a photovoltaic system mounted on it and fitted with a light flux collector system. For designing the optimum configuration of the photovoltaic converter, various technologies of market-available solar cell modules were considered, including silicon diffusion and

silicon heterojunction solar cells, featuring double- and single-sided designs. Analysis of the current development level of the photovoltaic industry suggests that a combination of silicon heterojunction solar cells with double-sided solar cell modules is the most promising from the viewpoint of energy conversion efficiency, technology simplicity and power generation convenience under real-life conditions.

For fabricating a high-performance solar power plant, a support structure was designed that allows 10 photovoltaic cell panels sized 1670 × 1000 mm^2 to be mounted on it, along with anodized aluminum light-reflecting surfaces having a reflection coefficient of above 0.94 used for intensifying the solar light flux incident upon the photovoltaic panels. The power plant also has stepper servomotors that rotate the light collecting system about the horizontal and vertical axes to permanently maintain the panel position perpendicular to the sunlight direction and hence deliver the highest energy production.

One of the key modules of the photovoltaic converter is the light-collecting concentrator system. The light-collecting system (Fig. 1) is an array of mirrors arranged at the optimum angle relative to the sunlight direction and reflecting sunlight to the solar panel mounted perpendicularly to the initial light flux. In this configuration the correct choice of the optimum reflecting material allows one to exclude the infrared fraction of the solar spectrum which mainly acts to heat up the working surfaces of solar cell modules. The light-collecting system is in the form of a rectangular frame sized 40 × 20 × 2 mm^2. The dimensions of the assembled light-collecting system are 1120 × 2100 × 1700 mm^3.

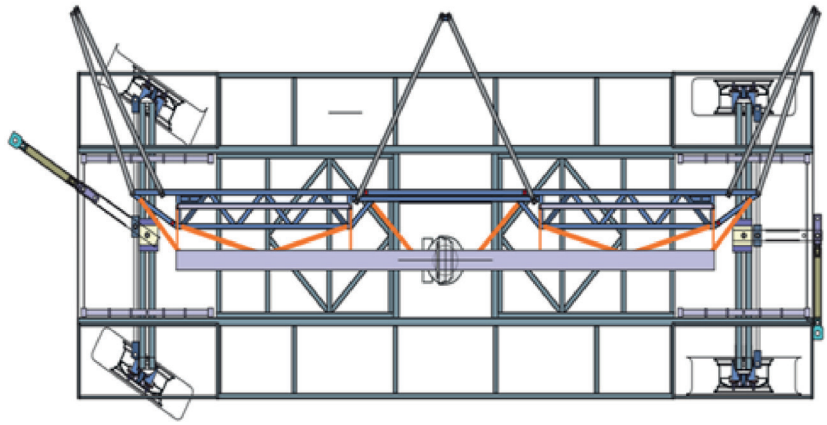

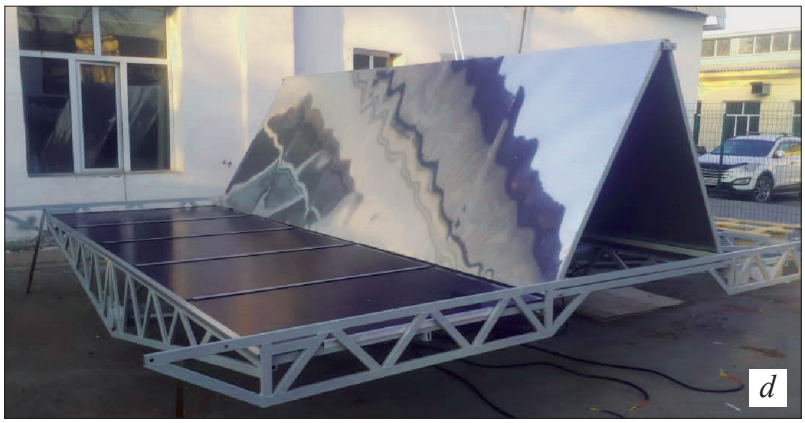

Figure 1. Configuration of light-collecting system for mobile photovoltaic converter on the basis of advanced solar cells: (*a*) general appearance, (*b*) photoelectric converter in expanded condition, (*c–d*) system assembly steps.

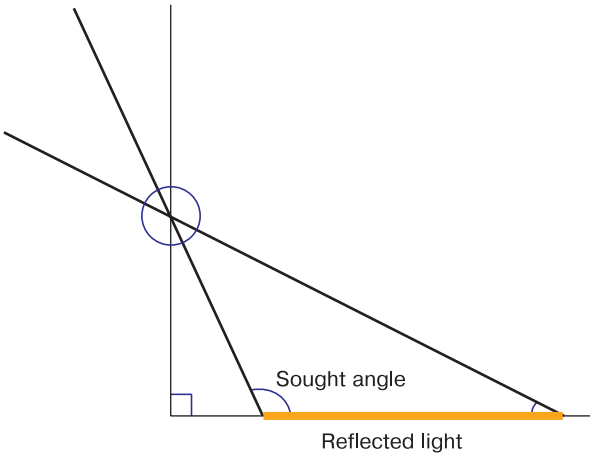

Figure 2. Geometrical interpretation of problem.

One of the tasks of system operation is to calculate the optimum angles at which the reflecting coatings are to be arranged relative to the solar panel. To calculate the optimum angle for the reflecting surfaces (mirrors) one should find the amount of light incident upon the solar panel from each of the mirrors depending on the sought angle. The initial conditions for solving this task were selected such that the problem transformed to a geometrical one where the sought parameter is the side of a triangle (Fig. 2). In this problem the lengths of the mirrors and the length of the solar cell module are equal.

Calculations showed that the sought triangle side is expressed as follows:

$$y^2(\mathrm{tg}^2(a) - 1 + 2y\cos(a) - 1 = 0, \tag{1}$$

where y is the function of reflected light and a is the mirror angle relative to solar cell module.

Whence in accordance with the Vieta's formulas one can find the solution and plot the graph of the function. Equation solutions can be found by solving the following set of equations:

$$\begin{cases} y_1 + y_2 = -\dfrac{2\cos(a)}{\mathrm{tg}^2(a)-1}, \\ y_1 \cdot y_2 = \dfrac{1}{1-\mathrm{tg}^2(a)}. \end{cases} \tag{2}$$

The solution of the above set of equations has following form:

$$y_1 = \frac{1}{\dfrac{-1+2\sin^2(a)}{-1+2\sin^2(a)}} \times \frac{\left[\cos^3(a) \mp \sqrt{\cos^6(a)+3\sin^3(a)-1-2\sin^4(a)}\right.}{-1+2\sin^2(a)} - \frac{2\sin^2(a)}{-1+2\sin^2(a)} \times \frac{\left.\left(\cos^3(a) \mp \sqrt{\cos^6(a)+3\sin^3(a)-1-2\sin^4(a)}\right)\right]}{-1+2\sin^2(a)} + \frac{2\cos(a)\sin^2(a)-2\cos(a)}{-1+2\sin^2(a)};$$

$$y_2 = \frac{\cos^3(a) \mp \sqrt{\cos^6(a)+3\sin^3(a)-1-2\sin^4(a)}}{-1+2\sin^2(a)}.$$

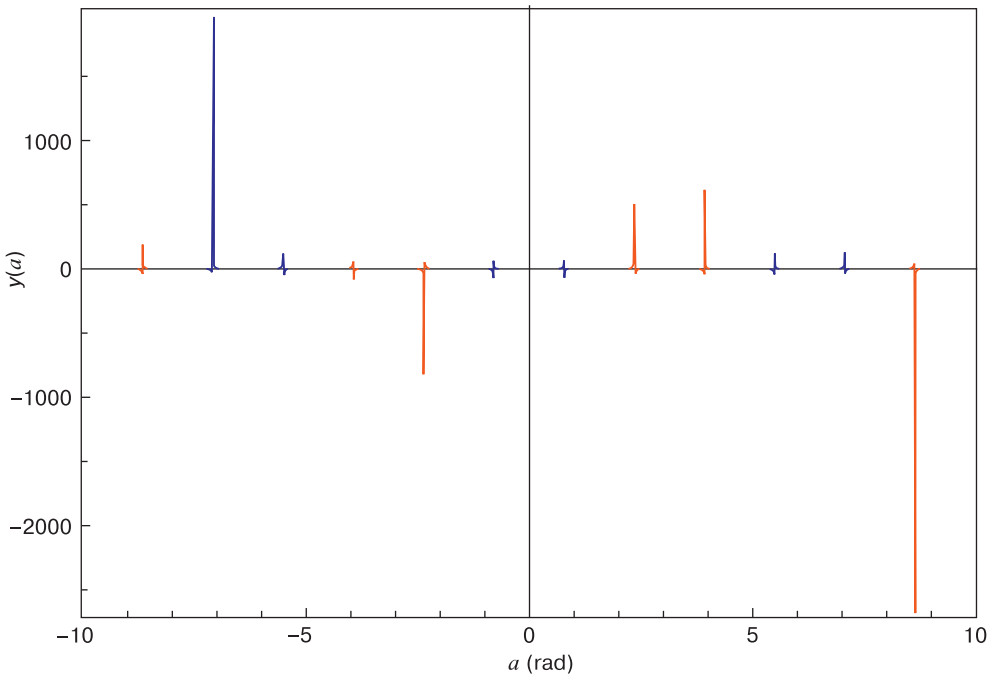

Figure 3. Graphical solution of Eq. (1).

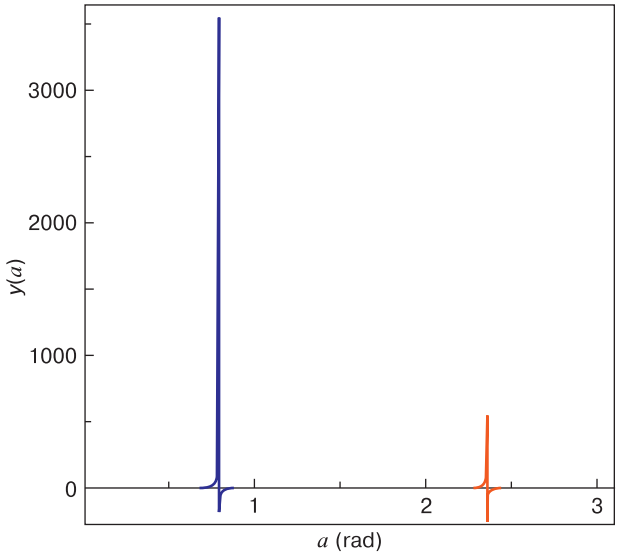

Figure 4. Graphical solution of Eq. (1) for the range of 0 to π.

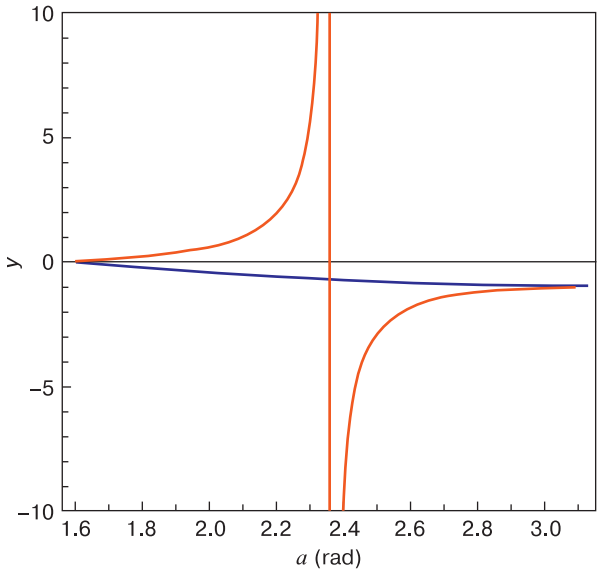

Figure 5. Graphical solution of Eq. (3).

The graphical solution has the form as illustrated in Fig. 3.

It can be seen from Fig. 3 that the solutions are a series of free-shaped curves. The range of interest is 0 to π (Fig. 4).

It can be seen from Fig. 4 that the values of the function tend to infinity at the angle a equal to 0.785 radian which corresponds to 45 arc deg. This means that light is reflected from the opposite side of the triangle in a direction parallel to the sought triangle side, but this case is disregarded for real-life conditions. However since we seek for mirror inclination angles of 90 arc deg or greater, we will consider the range of 90 to 180 arc deg. The solutions of Eq. (1) and the graphs (Figs. 3 and 4) suggest that the function y_1 already includes the solutions for the function y_2, but the y_2 solutions pertain to the range considered. Therefore the solution amounts to consideration of the function y_2:

$$y_2 = \frac{\cos^3(a) - \sqrt{\cos^6(a) + 3\sin^3(a) - 1 - 2\sin^4(a)}}{-1 + 2\sin^2(a)} \quad (3)$$

It can be seen from Fig. 5 that the values of the function start to increase after 90 arc deg and tend to infinity at an angle of 2.355 radian, i.e., 135 arc deg. The part of the graph in Fig. 5 located below the x axis suggests that at angles of higher than 135 arc deg the triangle side corresponding to the reflected light beams intersects with the base of the triangle in the left-hand side. This case is also disregarded because light is actually reflected only to one side, i.e., to the right-hand side (Fig. 2). We therefore determine the range of sought angles as 90 to 135 arc deg and the function range from 0.

The edge of the light spot reflected from the mirror edge which is the closest to the solar cell module changes its spatial position slower than the edge of the light spot reflected from the farther mirror side. Therefore the rate of the decrease in the size of the illuminated area is determined by the rate of the change in the position of the light spot reflected from the farther mirror side. Hence the rate of the decrease of the illuminated area size is equal to the rate of the growth of the function from 0 to 1. Since the function is symmetrical the sought expression meets the following function criterion:

$$f(a) = -y_2(a - (2.093 - 1.57)) + 10.$$

Therefore the sought function has the form $y(a) + f(a)$ (Fig. 7).

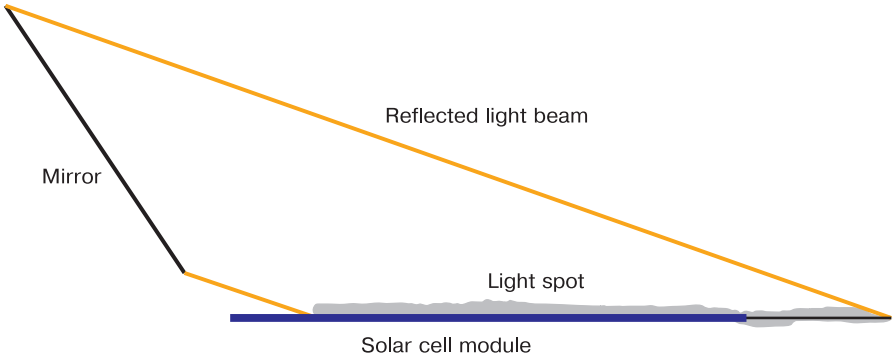

Figure 6. Reflected light beam path from mirror relative to solar cell module.

The solution illustrated in Fig. 7 is true for the case of two symmetrical mirrors. The sought optimum angle is 2.093 radian which is 120 arc deg. As can be seen from Fig. 7, the amount of reflected light starts to increase from an angle higher than 90 arc deg and continues until 120 arc deg. Then the amount of reflected light delivered to the solar cell panel starts to decrease.

SW PREMIUM PLUS HJT 310 photovoltaic cell panels were chosen, i.e., double-sided solar cell modules capable of producing up to 310 W under normal conditions (this work was actually carried out in 2019–2020, so currently we would probably consider using 400 W panels). Since it was planned to use double-sided panels the design output per panel could grow to 403 W for a 30% albedo case. Otherwise the output could be 582 W based on calculated data taking into account the light collecting system (without allowance for albedo). An array of 10 panels would then deliver an overall solar plant power of 5.8 kW (6.7 kW taking into account albedo). Thus a 7 kW power inverter would be suitable for this configuration.

Along with a high solar power plant output, the solar cell panel output parameters added to the inverter choice problem.

– V_{mpp} (maximum working output voltage): 36.1 V;

– I_{mpp} (maximum working output current) which for double illumination could grow to 8.6–17.2 A.

It is therefore clear that for an array of 10 panels connected in series the working voltage of the inverter should be as high as 361 V (without albedo). For a 7 kW solar power plant the only market-available suitable inverter models are expensive ones from foreign manufacturers, e.g. SMA. Furthermore these inverters are usually either only network-direct or can be only connected to storage batteries. However, the project was planned as a completely independent solar power plant capable of simultaneous network-direct AC power supply and battery operation, so the working parameters of these inverters did not satisfy the project requirements and moreover their price would start at $12k. Based on the design solar power plant parameters, several panel array options were considered (below are calculation data without albedo):

– 2 parallel strings of 5 panels, voltage to 181 V, current to 34.4 A;

– 3 parallel strings of 3 panels (with one backup module), voltage to 108.5 V, current to 51.6 A, maximum solar plant power to 5.26 kW.

Asymmetrical connection variants (e.g. 2 parallel strings of 4 or 6 panels) can also be used but their practical application often requires either an inverter with two separate contacts or two individual inverters.

After a market study the choice was made in favor of the MUST Power PV3500 PRO 8K inverter capable of simultaneous network-direct AC power supply and battery operation. The maximum input voltage from the photovoltaic modules is 145 V, the maximum current being 100 A. Thus the following connection diagram was chosen: 3 parallel strings of 3 panels with one backup panel.

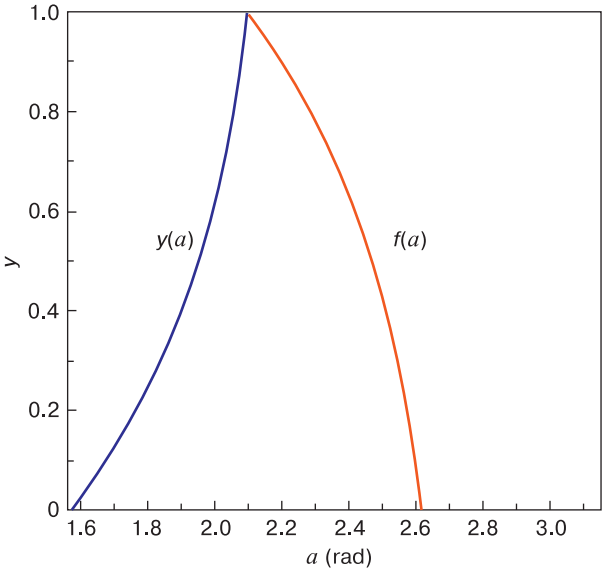

Figure 7. Graph of sought function.

A LED solar imitator was developed, assembled and started for testing of the photovoltaic panels. A specific feature of the solar imitator design was the possibility of testing conventional photovoltaic panels and double-sided ones.

The key requirement to the testing system developed is to provide accurate measurement data regardless of illumination conditions. The carriage on which the photovoltaic converter prototype is mounted can move inside the solar imitator enclosure. This design allows one to take readings of separate module or entire system parameters either at the illumination intensity “1 Sun” or at higher or lower illumination intensities.

The power source for the tests of the photovoltaic converter was a KEPCO BOP 50-20MG device with a maximum adjustable power of up to 1 kW. The KEPCO BOP device series are programmable power units having adjustable power source and consumption (load) functionality. This combination of power source and load functionality allows one to simulate tests of photovoltaic converter systems under real environmental conditions. This approach allows measuring both the effective electrical parameters of photovoltaic systems and parameters obtained in laboratory setup.

Achieving the highest solar cell panel efficiency requires correct choice of load resistance. To this end the photovoltaic panels are not connected to the load directly but via a photoelectric system controller which is used to provide for the optimum solar cell panel operation mode.

The measuring system incorporated into the adjustable power source and into the LED solar imitator allows selecting the required conditions and controllers for the optimum operation of the photovoltaic panels. The adjustable power source allows not only measuring the VACs of the tested solar cell modules but also imitating critical operation conditions by varying the load and simulating strong power surges, whereas the LED solar imitator allows imitating either low illumination conditions of the

solar cell module or an above "1 Sun" illumination intensity. The LabVIEW software is used for data processing.

For the in-the-field tests of the photovoltaic converter, the wind load exerted onto the test solar cell converters was calculated. The following calculations were conducted: load summary, structure natural vibration frequency evaluation, support strength assessment and approximate support anchor bolt strength calculation. All the calculations were presented as xlsx spreadsheet format scripts. For wind load calculation one can use the respective xlsx format script to ensure durable assembly of the photoelectric converters and develop appropriate recommendations for farmers as to system orientation relative to the prevailing winds and wave-break installation. These calculations are not included into this work since they are based on commonly known methods and do not constitute any scientific interest.

The DC cable interconnecting the modules and the inverter was chosen based on a permitted current load of max. 4 A per 1 mm^2 wire section. Special outdoor installation glass-fiber insulated cable with a 16 mm^2 conductor section was chosen. At the maximum possible current of 51.6 A the current load per 1 mm^2 conductor section does not exceed 3.23 A. In this case the voltage loss per 100 m cable is max. 11% which is considered to be a very good result at the loads expected.

The choice of battery was based on only one criterion, i.e., the overall battery capacity must be capable of supporting 24 h independent power plant operation. The battery capacity was finally chosen based on the typical power consumption of the target user, e.g. a farmer or a shepherd. A total of 8 MUST helium batteries with a capacity of 250 A · h each were acquired.

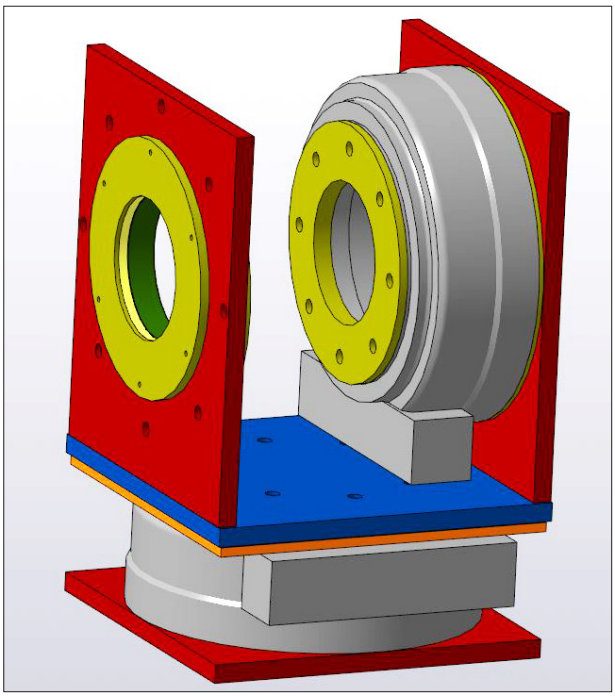

Figure 8. SE9 stepper motor drive.

The stepper servomotors were chosen to be SE9 slewing drives with a stepper motor (Fig. 8) having a 6.5 kN · m torque and a 33.9 kN · m steady state torque.

The converter design uses a two-axis tracker system for the general case of planar solar cell module mounting. A 350 mm stroke drive provides for movement in the north-south direction and a 450 mm stroke drive, in the east-west direction. The task was to find the required arm for providing symmetrical positioning at the maximum rotation angle about the axis. As a result, technical solutions were developed for the north-south and the east-west directions.

Furthermore a wiring schematic diagram was designed to implement the preset solar tracking system algorithm. The system is fitted with a GPS/GLONASS module for system precision positioning and time synchronization.

3. Conclusion

A unit was designed and fabricated comprising an array of mirrors arranged at the optimum angle relative to the light flux direction and reflecting the solar radiation to a solar panel installed perpendicularly to the initial light flux. Mathematical simulation was used for finding the optimum inclination angle of the reflecting surface for the suggested design of a light accumulating and concentrating system. The sought optimum angle was 2.093 radian which is 120 arc deg. At higher angles the amount of reflected light delivered to the solar cell panel starts to decrease.

A two-axis tracker system was developed for the general case of planar solar cell module mounting. A 350 mm stroke drive provides for movement in the north-south direction and a 450 mm stroke drive, in the east-west direction. The task was to find the required arm for providing symmetrical positioning at the maximum rotation angle about the axis. As a result, technical solutions were developed for the north-south and the east-west directions.

A microcontroller based schematic wiring diagram was designed to implement the preset solar tracking system algorithm. The system is fitted with a GPS/GLONASS module for system precision positioning and time synchronization.

Another technical solution currently developed by the Authors team is a steady-state mobile solar power plant. The mobile solar power plant delivers shepherd power support during fast flock transfer within fenced pasture segments. The system will be furnished to consumers with the complete set of fittings and ready for operation. The plant design is transformable, with all the equipment sets being universal and suitable for fast and easy installation where required. The electrical components of the power plant are preassembled and also ready for operation. The batteries and the control unit (charge and voltage controller) are provided integral in a cubicle having all receptacles suitably located on its front panel. The working configuration of the output circuit is coupled with a gasoline

generator which can be switched on in case of emergency power outage. The output power of the plant's photovoltaic converters will be designed based on expected loads. The solar power plant can be used to power electrically driven water pumps, video control systems, electric lighting, mechanical devices including shredders, fodder crushers etc.. All the electric equipment will be assembled in a weather-protected enclosure, with the solar cells located on top the enclosure. The novelty of this design is that "smart house" components will for the first time be used for agricultural purposes in Kazakhstan.

Acknowledgments

The Authors are grateful to the Ministry of Education and Science of the Republic of Kazakhstan for project funding, No. AP09259279.

References

1. Energy Jordan. EES EAEC. World Energy. https://www.eeseaec.org/energetika-stran-mira/energetika-iordanii
2. Al-Saidi M., Lahham N. Solar energy farming as a development innovation for vulnerable water basins. *Development in Practice*. 2019; 29(5): 619–634. https://doi.org/10.1080/09614524.2019.1600659
3. Majewski J., Szymanek M. Technical, economic and legal conditions of the development of photovoltaic generation in Poland. *Acta Energetica.* 2012; 2(11): 21–26.
4. Swanson R.M. The promise of concentrators. *Progress in Photovoltaics: Research and Application*. 2000; 8(1): 93–104. https://doi.org/10.1002/(sici)1099-159x(200001/02)8:13.0.co
5. Photovoltaic device performance calibration services. https://pvdpc.nrel.gov/ (accessed on 22.08.2019).
6. Andreev V.M. Concentrator solar photovoltaics. *Al'ternativnaâ ènergetika i èkologiâ = Alternative Energy and Ecology (ISJAEE).* 2012; (5-6): 40–44. (In Russ.)
7. Alferov Zh.I., Andreev V.M., Rumyantsev V.D. Solar photovoltaics: trends and prospects. *Fizika i Tekhnika Poluprovodnikov = Physics and Technology of Semiconductors*. 2004; 38(8): 937–948. (In Russ.)
8. Andreev V.M., Grilikhes V.A., Rumyantsev V.D. Photovoltaic conversion of concentrated sunlight. John Wiley & Sons Ltd; 1997. 312 p.
9. Andreev V.M., Khvostikov V.P., Rumyantsev V.D., Paleeva E.V., Shvarts M.Z., Algora C. *Proc.of the 24th Linear Accelerator Meeting*. Japan, Sapporo. July 7–9, 1999. 147 p.
10. Green M.A., Emery K., Hishikawa Y., Warta W., Dunlop E.D. Solar cell efficiency tables (version 42). *Progress in Photovoltaics*. 2013; 21(5): 827–837. https://doi.org/10.1002/pip.2404
11. Green M.A., Emery K., Hishikawa Y., Warta W., Dunlop E.D. Solar cell efficiency tables (version 43). *Progress in Photovoltaics*. 2014; 22(1): 1–9. https://doi.org/10.1002/pip.2452
12. Sawada T., Terada N., Tsuge S., Baba T., Takahama T., Wakisaka K., Tsuda S., Nakano S. High-efficiency a-Si/c-Si heterojunction solar cell. *Proc. of 1994 IEEE 1st World Conf. on Photovoltaic En. Conversion – WCPEC (A Joint Conf. of PVSC, PVSEC and PSEC)*. Waikoloa, HI, USA. 5–9 Dec., 1994. USA: IEEE; 1994: 1219–1226. https://doi.org/10.1109/WCPEC.1994.519952
13. Yamamoto K. 25.1% efficiency Cu metallized heterojunction crystalline Si solar cell. *25th Int. Photovoltaic Sc. and Eng. Conf.* Busan, Korea. November, 2015.
14. Dimroth F., Tibbits T., Niemeyer M., Predan F., Beutel P., Karcher C., Oliva E., Siefer G., Lackner D., Fus-Kailuweit P., Bett A., Krause R., Drazek C., Guiot E., Wasselin J., Tauzin A., Signamarcheix T. Four-junction wafer-bonded concentrator solar cells. *IEEE Journal of Photovoltaics*. 2015; 6(1): 343–349. https://doi.org/10.1109/PVSC.2015.7356148
15. Geisz JF, Steiner MA, Jain N, Schulte K., France R., McMahon W., Perl E., Friedman D.Building a six-junction inverted metamorphic concentrator solar cell. *IEEE Journal of Photovoltaics*. 2018;8(2):626–632. https://doi.org/10.1109/JPHOTOV.2017.2778567
16. Sharp develops concentrator solar cell with world's highest conversion efficiency of 43.5%: Achieved with concentrator triple-junction compound solar cell. Press release Sharp Corporation. May 31, 2012. http://sharp-world.com/corporate/news/120531.html
17. Slade A., Garboushian V. 27.6% efficient silicon concentrator cell for mass production. *Techn. Digest. 15th Inter. Photovoltaic Sc. and Eng. Conf*. Beijing, October 11–13; 2005. 701 p. https://www.researchgate.net/publication/267779112_276_Efficient_Silicon_Concentrator_Solar_Cells_for_Mass_Production
18. Ward J.S., Ramanathan K., Hasoon F.S., Coutts T.J., Keane J., Contreras M.A., Moriarty T., Noufi R.A. 21.5% efficient Cu (In,Ga) Se_2 thin-film concentrator solar cell. *Progress in Photovoltaics Research and Application.* 2002; 10(1): 41–46. https://doi.org/10.1002/pip.424
19. Chiang C.J., Richards E.H. A twenty percent efficient photovoltaic concentrator module. *Proc. IEEE Conf. on Photovoltaic Specialists*. Kissimmee, FL, USA. 21–25 May, 1990. IEEE: 861–863. https://doi.org/10.1109/PVSC.1990.111743
20. Yoshikawa K., Kawasaki H., Yoshida W., Irie T., Konishi K., Nakano K., Uto T., Adachi D., Kanematsu M., Uzu H., Yamamoto K. Silicon heterojunction solar cell with interdigitated back contacts for a photoconversion efficiency over 26%. *Nature Energy*. 2017; 2(5): 17032. https://doi.org/10.1038/NENERGY.2017.32
21. Tokmoldin N.S., Chuchvaga N.A., Zholdybayev K.S., Terukov E.I., Tokmoldin S.Z., Verbitskii V.N., Titov A.S. The use of solar cells with a bifacial contact grid under the conditions of Kazakhstan. *Technical Physics*. 2017; 62(12): 1877–1881. https://doi.org/10.1134/S106378421712026X
22. López A.L., Andreev V.M. (eds.). Silicon concentrator solar cells. In: *Concentrator photovoltaics*. Vol. 130. Springer series in optical sciences. Heidelberg, Berlin: Springer; 2007: 51–66. https://doi.org/10.1007/978-3-540-68798-6_3